



HAL
open science

Inferring Population Histories Using Genome-Wide Allele Frequency Data

Mathieu Gautier, Renaud Vitalis

► **To cite this version:**

Mathieu Gautier, Renaud Vitalis. Inferring Population Histories Using Genome-Wide Allele Frequency Data. *Molecular Biology and Evolution*, 2012, 30 (3), pp.654-668. 10.1093/molbev/mss257 . hal-00783026

HAL Id: hal-00783026

<https://hal.science/hal-00783026>

Submitted on 14 Jun 2021

HAL is a multi-disciplinary open access archive for the deposit and dissemination of scientific research documents, whether they are published or not. The documents may come from teaching and research institutions in France or abroad, or from public or private research centers.

L'archive ouverte pluridisciplinaire **HAL**, est destinée au dépôt et à la diffusion de documents scientifiques de niveau recherche, publiés ou non, émanant des établissements d'enseignement et de recherche français ou étrangers, des laboratoires publics ou privés.



Distributed under a Creative Commons Attribution 4.0 International License

Inferring Population Histories Using Genome-Wide Allele Frequency Data

Mathieu Gautier^{*1,2} and Renaud Vitalis^{1,2,3}

¹INRA, UMR CBGP (INRA – IRD – Cirad – Montpellier SupAgro), Campus international de Baillarguet, Montferrier-sur-Lez, France

²Institut de Biologie Computationnelle, 95 rue de la Galéra, 34095 Montpellier, France

³Institut des Sciences de l'Évolution, UMR 5554, CNRS, Université Montpellier 2, Montpellier, France

***Corresponding author:** E-mail: Mathieu.Gautier@supagro.inra.fr.

Associate editor: Noah Rosenberg

Abstract

The recent development of high-throughput genotyping technologies has revolutionized the collection of data in a wide range of both model and nonmodel species. These data generally contain huge amounts of information about the demographic history of populations. In this study, we introduce a new method to estimate divergence times on a diffusion time scale from large single-nucleotide polymorphism (SNP) data sets, conditionally on a population history that is represented as a tree. We further assume that all the observed polymorphisms originate from the most ancestral (root) population; that is, we neglect mutations that occur after the split of the most ancestral population. This method relies on a hierarchical Bayesian model, based on Kimura's time-dependent diffusion approximation of genetic drift. We implemented a Metropolis–Hastings within Gibbs sampler to estimate the posterior distribution of the parameters of interest in this model, which we refer to as the Kimura model. Evaluating the Kimura model on simulated population histories, we found that it provides accurate estimates of divergence time. Assessing model fit using the deviance information criterion (DIC) proved efficient for retrieving the correct tree topology among a set of competing histories. We show that this procedure is robust to low-to-moderate gene flow, as well as to ascertainment bias, providing that the most distantly related populations are represented in the discovery panel. As an illustrative example, we finally analyzed published human data consisting in genotypes for 452,198 SNPs from individuals belonging to four populations worldwide. Our results suggest that the Kimura model may be helpful to characterize the demographic history of differentiated populations, using genome-wide allele frequency data.

Introduction

The recent development of high-throughput genotyping technologies has revolutionized the collection of data in a wide range of both model and nonmodel species. These data, which may involve tens to hundreds of thousands of single-nucleotide polymorphisms (SNPs) in humans (Jakobsson et al. 2008; Li et al. 2008) and other model species (Gautier, Laloë, et al. 2010; Kijas et al. 2012), contain huge amounts of information about the demographic history of populations (Wang and Nielsen 2012). By efficiently reducing multidimensional genetic data into a few synthetic variables, multivariate analyses (see Jombart et al. 2009, for a review) such as principal component analyses have proven useful to summarize available information about population structure (Patterson et al. 2006; Novembre et al. 2008; Gautier, Laloë, et al. 2010). However, because they are exploratory and model free, such approaches are not aimed at making inferences about the underlying history of populations (but see McVean [2009], for a coalescent interpretation of principal components). Alternatively, model-based approaches have been developed to infer the population structure from multi-locus genotypes. One of the most popular, which has been implemented in the software package *structure* (Pritchard et al. 2000), performs a clustering of individuals into genetically homogeneous groups based on an explicit population genetic model (see also Tang et al. 2005; Alexander et al.

2009). It allows not only the assignment of individuals into genetically homogeneous clusters (sometimes interpreted as ancestral populations) but also the estimation of parameters like the (unknown) allele frequencies in each cluster or the admixture proportions for each individual. However, a limitation of both multivariate analyses and clustering methods is that they are only aimed at characterizing the genetic structure of populations. They do not provide any clue regarding the historical processes that caused the observed structure.

A convenient way of representing the demographic history of populations is borrowed from phylogenetics (Felsenstein 2003). It is based on the idea that the historical relationship between populations can be represented as a multifurcating diagram or a “tree.” The terminal nodes, or leaves, of the tree represent the present-day populations, whereas the internal nodes are interpreted as ancestral (unobserved) populations. The branch length between any two nodes is proportional to the amount of genetic divergence between the corresponding populations. Early attempts to characterize population trees relied on moment-based methods to infer the tree topology and to obtain estimates of the branch lengths (Saitou and Nei 1987). In principle, likelihood-based techniques are more efficient in using the information present in the genetic data. However, they require the definition of a stochastic model to compute the likelihood of a sample of genes, which is expressed as a function of some parameters that characterize

the topology and the branch lengths of a population tree. Two categories of approaches have been followed to derive such likelihood. These differ in whether genetic drift is approximated as a backward-in-time (coalescent) process or as a forward-in-time (diffusion) process.

The first approach, based on coalescent theory (Kingman 1982), provides the probabilistic framework to compute the likelihood of a sample of genes, conditional on the (unknown) genealogy of that sample (Hein et al. 2005; Wakeley 2008). Because it can only be computed for a single genealogical history and because many such histories are compatible with the data, Markov chain Monte Carlo (MCMC) algorithms have been developed to integrate over unknown genealogies (Hey and Nielsen 2004, 2007). However, the convergence of these algorithms can be very difficult to achieve, particularly as the sample size increases and scenarios are more complex (Marjoram and Tavaré 2006; Beaumont 2008; Wakeley 2008). The second approach, to which this study belongs, is based on diffusion theory (Kimura 1964). It consists in approximating the discrete process of genetic drift by a continuous-time diffusion process. Applications of diffusion theory provide a probability density of allele frequencies in some simple population models (Kimura 1964; Ewens 2004), which can then be used to compute the likelihood of a sample of genes.

In the absence of migration, genetic drift occurs independently in each branch of a population tree. Let us consider one particular branch, with effective population size N . At one SNP locus, the allele frequencies drift from one generation to the next, so that, in the absence of mutation, the number $X(t+1)$ of copies of one allele at generation $t+1$ is a binomial random variable with index $2N$ and parameter $X(t)/2N$. In this so-called Wright–Fisher model, starting from an ancestral frequency π , the expected allele frequency $\alpha(t)$ of that allele after t generations is unchanged: $\mathbb{E}[\alpha(t)] = \pi$, and its variance is $\text{Var}_{\text{WF}}[\alpha(t)] = F\pi(1-\pi)$, where $F = 1 - (1 - \frac{1}{2N})^t$ is a measure of divergence between the ancestral and the current population (Wright 1969, p. 345–346). Although deriving explicit formulas for the whole distribution of allele frequencies in the Wright–Fisher model proves to be difficult (Ewens 2004), it is possible to accurately approximate this discrete process by a continuous-time diffusion process. This diffusion approximation is based on a change of time scale whereby infinitesimal changes in gene frequencies occur every $\delta t \equiv 1/2N$ units of time (Crow and Kimura 1971; Ewens 2004). Hence, the unit of time in the diffusion process corresponds to $2N$ generations in the discrete-time model. Using a diffusion approximation to the one-locus, two-alleles Wright–Fisher process, Gutenkunst et al. (2009) proposed a new method to infer population history in models involving up to three populations. Their method, implemented in the software package *∂a∂i*, is based on numerical computation of the expected joint frequency spectrum within and between populations. Numerical evaluation of the diffusion approximation of the joint frequency spectrum allows considering complex evolutionary scenarios including expansions, contractions, migrations, etc. However, the generality of the approach comes at the cost of computational burden.

Hence, although *∂a∂i* handles large resequencing data sets (several Mb), it is limited by the number of populations analyzed. In the Wright–Fisher model, Kimura (1964) derived a general solution, in the absence of selection and mutation, for the distribution of allele frequencies in a finite-size population at any time t . In principle, this solution may be used to compute the likelihood of a sample of genes, which paves the way for the inference of the model parameters. However, because Kimura’s (1964) expression, which depends on some hypergeometric functions, is notoriously difficult to compute (Wang and Rannala 2004), its use in likelihood-based inference for large genetic data sets has been extremely limited so far.

Instead, several approximations to the pure-drift divergence process have been sought to facilitate the computation of the likelihood of population trees and estimate the underlying parameters. Cavalli-Sforza and Edwards (1967) approximated genetic drift as a Brownian motion process through arc-sine square root transformation of allele frequencies. Very efficient algorithms based on this approximation have been developed, which have been extensively used in the context of maximum-likelihood inference of population trees (see Felsenstein 2003, p. 410–414). However, the Brownian motion approximation is only valid for small divergence times. Recently, Siren et al. (2011) proposed to reconstruct population histories from a combination of analytical, numerical, and Monte Carlo integration techniques based on a beta approximation of the allele frequency distribution, with expectation π and variance $F\pi(1-\pi)$. Even more recently, Pickrell and Pritchard (2012) developed a statistical model for inferring population splits and mixtures, based on a multivariate generalization of the Gaussian approximation of the allele frequency distribution (Coop et al. 2010). Approximating the allele frequency distribution by a Gaussian distribution with mean π and variance $F\pi(1-\pi)$ was originally suggested by Nicholson et al. (2002). However, although the Gaussian and the beta distributions have the same expectation and variance as predicted in the Wright–Fisher model, neither can be derived from first principles in this model. In that respect, both models are reminiscent of Cavalli-Sforza and Edwards’s (1967) approach, in the sense that they are based on mathematically convenient instrumental distributions, rather than on the diffusion approximation of the process at play.

With the advent of computing power, though, the calculation of complex expressions in likelihood-based inference techniques is now within reach, even for large data sets. In this study, we therefore use Kimura’s (1964) diffusion approximation to estimate divergence times from large SNP data sets, conditionally on a population history that is represented as a tree. We further assume that all the observed polymorphisms originate from the most ancestral (root) population, that is, we neglect mutation. This method is based on a hierarchical Bayesian model, for which we implemented a Metropolis–Hastings within Gibbs sampler to estimate the posterior distribution of the parameters of interest, namely the branch lengths throughout the population tree. We evaluated our method using simulated population histories, accounting for

various departures from the model assumptions (gene flow and ascertainment bias). Because the true population history is usually unknown, we further investigated the use of the deviance information criterion (DIC) (Spiegelhalter et al. 2002) for choosing between alternative population histories. As an application example, we finally reanalyzed published human data consisting in genotypes for 452,198 SNPs from individuals belonging to four human populations worldwide (Jakobsson et al. 2008).

New Approaches

The Kimura Statistical Model

In the following, we derive a hierarchical Bayesian model for integrating gene frequencies in a population tree. Consider a sample made of J populations sharing a common history. Each population has a label, k , which varies from 1 to J for the sampled populations, and from $J + 1$ to r for the internal nodes of the tree, where r represents the population at the root of the tree. For a bifurcating tree, there are $J - 1$ internal nodes and therefore $r = 2J - 1$. For a star-shaped phylogeny, where all sampled populations derive from a single ancestral population, $r = J + 1$. In the following, we note $a(k)$ the ancestral population of population k . The directed acyclic graph of the model is provided in figure 1, where the annotations are given for illustrative purposes in the special case of a bifurcating tree with three populations. The data consist in l SNP loci, which are biallelic markers with an ancestral and a derived allelic state. In the following we consider a reference allele, which is arbitrarily defined (e.g., by randomly drawing the ancestral or the derived state). Let n_{ij} be the total number

of genes sampled at the i th locus ($1 \leq i \leq l$) in the j th population ($1 \leq j \leq J$), that is, twice the number of genotyped individuals in a diploid population. Let x_{ij} be the observed count of the reference allele at the i th locus in the j th sampled population. Assuming Hardy–Weinberg Equilibrium, the conditional distribution of x_{ij} given n_{ij} and the true (yet unknown) allele frequency α_{ij} is binomial:

$$x_{ij} \mid n_{ij}, \alpha_{ij} \sim_{iid} B(\alpha_{ij}, n_{ij}). \tag{1}$$

Let us now consider the second level of the hierarchical model (fig. 1), which integrates over the distribution of the reference allele frequencies α_{ik} at the i th SNP in the k th population ($k < r$). In the absence of mutation, assuming that population k with effective size N_k diverged from $a(k)$ for t_k discrete nonoverlapping generations, the distribution of α_{ik} , conditional upon the allele frequency $\alpha_{ia(k)}$ in the parental population, and upon the branch length $\tau_k \equiv t_k/(2N_k)$, reads:

$$\left\{ \begin{aligned} \pi(\alpha_{ik} \mid \alpha_{ia(k)}, \tau_k) &= (1 - w_{ik}^2) \sum_{l=1}^{\infty} \frac{2l+1}{l(l+1)} T_{l-1}^1(w_{ik}) T_{l-1}^1(z_i) e^{-\frac{1}{2}(l+1)\tau_k} \quad \text{if } 0 < \alpha_{ik} < 1 \\ P(\alpha_{ik} = 0 \mid \alpha_{ia(k)}, \tau_k) &= (1 - \alpha_{ia(k)}) + \frac{(1-z_i)^2}{2} \sum_{l=1}^{\infty} (-1)^l \frac{2l+1}{l(l+1)} T_{l-1}^1(-z_i) e^{-\frac{1}{2}(l+1)\tau_k} \\ P(\alpha_{ik} = 1 \mid \alpha_{ia(k)}, \tau_k) &= \alpha_{ia(k)} + \frac{(1-z_i)^2}{2} \sum_{l=1}^{\infty} (-1)^l \frac{2l+1}{l(l+1)} T_{l-1}^1(z_i) e^{-\frac{1}{2}(l+1)\tau_k} \end{aligned} \right. , \tag{2}$$

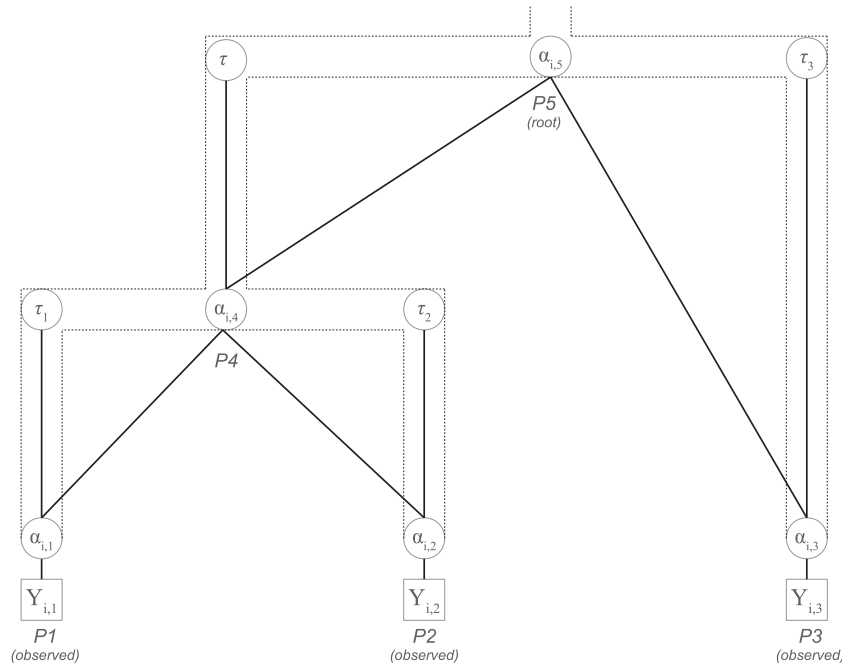


Fig. 1. Directed acyclic graph (DAG) of the hierarchical Bayesian model for an example tree with $J = 3$ populations. The topology ((P1,P2),P3) is represented in gray. Y_{ij} represents the observed count of the reference allele at the i th SNP in population j , and α_{ij} is its (unknown) frequency in that population. The parameter $\tau_j \equiv t/N_j$ is the length (on a diffusion time scale) of the branch leading to population j . Following our notations (see the main text), the observed populations (P1, P2, and P3) are indexed from $j = 1$ to $j = J = 3$. The (unobserved) population ancestral to P1 and P2 is indexed by $a(1) = a(2) = 4$, and the (unobserved) population that is ancestral to P3 and P4 (root population) is indexed by $r = a(3) = a(4) = 5$.

(see formulae 4.9 and 4.16 in Kimura [1964]). In equation (2), $w_{ik} = 1 - 2\alpha_{ik}$ and $z_i = 1 - 2\alpha_{ia(k)}$; $T_{l-1}^1(x)$ denotes the Gegenbauer polynomial, which can be computed using the recursion: $T_0^1(x) = 1$, $T_1^1(x) = 3x$, ..., and $T_n^1(x) = \frac{1}{n} [(2x(n + \frac{1}{2})T_{n-1}^1(x) - (n+1)T_{n-2}^1(x))]$ for $n \geq 2$. In practice, the Gegenbauer polynomial was computed using an iterative algorithm checking for convergence for two consecutive iterations. Convergence was generally achieved within 30 iterations, except for low divergence (e.g., $\tau_k < 0.02$) whereby a few hundreds iterations could be needed.

Although it is possible in theory to integrate the binomial sampling over the first level of the hierarchy (i.e., over the α_{ik} for $k = 1$ to $k = J$; see the [supplementary materials](#), [Supplementary Material](#) online), we found that the evaluation of the resulting formula was numerically unstable and was not efficient computationally (data not shown).

As the allele frequencies in the ancestral population of the full sample ($k = r$) are unknown, we assumed that the prior distribution of the frequency α_{ir} of the reference allele for the i th SNP follows a beta distribution:

$$\alpha_{ir} \sim_{iid} \text{Beta}(1.0, 1.0). \tag{3}$$

This prior is noninformative in the sense of the indifference principle, which assigns equal probabilities to all possibilities.

Finally, the divergence parameter τ_k 's are assumed to be sampled from a uniform distribution:

$$\tau_k \sim_{iid} \mathcal{U}(0, 10). \tag{4}$$

Assuming that genetic drift occurs independently in each branch of the tree, we may characterize the gene frequency hierarchically along the tree from the most ancestral population toward the leaves. The full model (fig. 1) then takes the form:

$$\begin{aligned} \pi(\alpha, \tau | \mathbf{x}) \propto & \left[\prod_{i=1}^{i=l} \prod_{j=1}^{j=l} P(x_{ij} | \alpha_{ij}) \right] \\ & \times \left[\prod_{j=1}^{j=r-1} \pi(\tau_j) \prod_{i=1}^{i=l} \pi(\alpha_{ij} | \alpha_{ia(j)}, \tau_j) \right] \prod_{i=1}^{i=l} \pi(\alpha_{ir}). \end{aligned} \tag{5}$$

Results

Precision of the Kimura Model for Estimating Differentiation in the Wright–Fisher Model

To analyze the precision of the Kimura model based on Kimura's diffusion approximation, we first analyzed simulated data consisting of allele counts at 5,000 SNPs genotyped from four populations having diverged simultaneously from a single ancestral population (star-shaped phylogeny). As the truncated Gaussian model (Nicholson et al. 2002) and the beta model (Balding and Nichols 1995) have been used to approximate genetic drift in star-shaped population histories (see, e.g., Gautier, Hocking, et al. 2010), we analyzed these simulated data sets using previously described programs based on these two models (Gautier, Hocking, et al. 2010). For the truncated Gaussian and the beta models, branch lengths were interpreted in terms of a differentiation

parameter $F_k \in (0, 1)$, which corresponds to a population-specific F_{ST} (Weir and Hill 2002; Excoffier 2007). Following the notations and assumptions made earlier, $F_k = 1 - [1 - 1/(2N_k)]^t$ (Wright 1969, p. 345–346). Hence, providing N_k is not too small (e.g., $N_k > 50$) and τ_k is not too large (e.g., $\tau_k < 0.15$), then $F_k \approx \tau_k$ (fig. 2B and C). Twenty-three temporal samples (from $t = 0.01$ to $t = 1$ unit of time) were taken to assess the precision of the estimations as a function of the level of differentiation. The Kimura model provided very good estimates of divergence times [$\tau_k \equiv t/(2N_k)$], irrespectively of the level of differentiation (fig. 2A). Conversely, and as already observed (Gautier, Hocking, et al. 2010), both the truncated Gaussian model (fig. 2B) and the beta model (fig. 2C) provided upwardly biased estimates for F_k when τ_k exceeded 0.2. For the beta model, though, biased estimates of F_k were close to τ_k as long as $\tau_k < 0.5$ (fig. 2C).

We further evaluated the performance of the Kimura model to estimate branch lengths in bifurcating trees. To that end, allele count data for 5,000 SNPs were simulated for three populations (denoted as P1, P2, and P3) related by the same topology ((P1,P2),P3) but with varying branch lengths. Fifty replicates per history were performed. As illustrated in figure 3, the Kimura model provided accurate estimates of divergence times even if a slight-to-moderate bias was observed for the internal branch (leading to population P4 in the simulated scenarios). The bias was more pronounced with smaller divergence time (fig. 3D).

Performance of the Kimura Model to Characterize Population History

Fifty data sets consisting in allele counts at 5,000 SNPs were simulated using *ms* coalescent-based simulations for a three-population history noted T1 in figure 4. Each data set was then analyzed conditionally on the four possible tree topologies represented in figure 4 and denoted by T1, T2, T3, and S. As mentioned earlier, T1 corresponded to the true (simulated) history, T2 and T3 corresponded to incorrect histories, and S corresponded to a star-shaped (also incorrect) history.

We found that, across replicated simulated data sets, the DIC always provided a clear support in favor of the correct population history (table 1). However, the power of the DIC to identify the correct tree was strongly dependent on the information available in the data sets. Indeed, as presented in table 2, for small data sets (1,000 SNPs), the DIC criterion provided support for an incorrect tree topology in a substantial number of cases, whereas for reasonably larger data sets (including 5,000 or 25,000 SNPs), the DIC was always supporting the correct tree topology. Similarly, the average difference in DIC across replicates between the correct and alternative tree topologies increased sharply with the number of SNPs in the data sets. Finally, for any given number of SNPs, the power of the DIC to support the correct population history slightly decreased with the number of populations considered, and the complexity of the tree topology, as illustrated in [supplementary figures S1 and S2](#), [Supplementary Material](#) online.

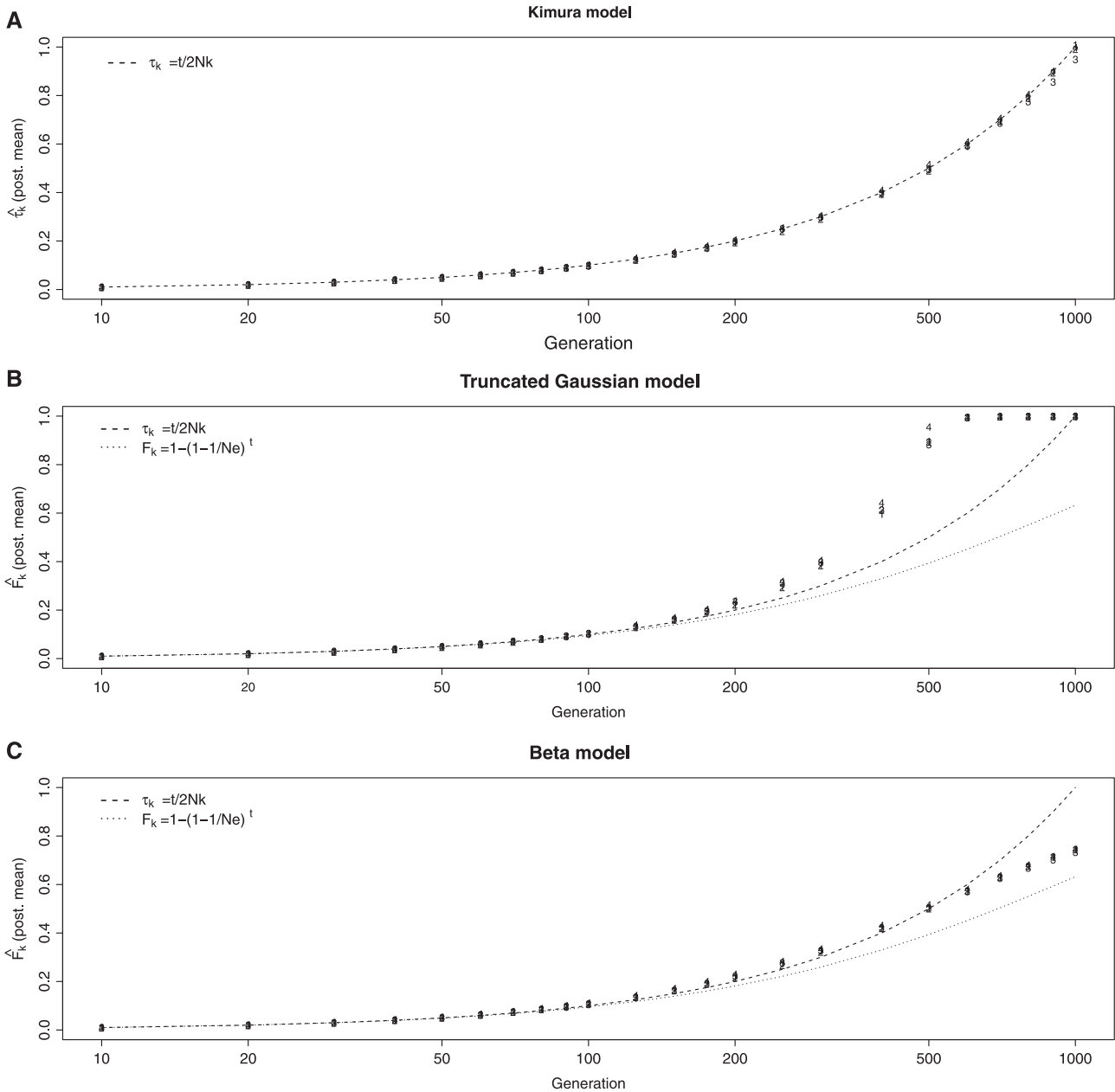


Fig. 2. Estimating branch lengths in star phylogenies with four populations. The posterior means of each of the four branch lengths were estimated with the Kimura model in terms of divergence on a diffusion time scale τ_k (A). With the truncated Gaussian and the beta models (graphs B and C, respectively), divergence was measured as F_k , which corresponds to a population-specific F_{ST} . The data sets consisted in 5,000 SNPs sampled from four populations diverging simultaneously from their common ancestor (star-shaped phylogeny). The data were collected at 24 different time points after divergence (see the main text for further details). In (A), (B), and (C), the dashed lines indicate the (true) divergence time on the diffusion time scale (here, $\tau_k \equiv t/(2N_e)$ where $N_e = 500$ is the [diploid] effective population size). In (B) and (C), the dotted lines indicate the (true) value of the population-specific F_{ST} ($F_k = 1 - [1/(2N_e)]^t$). Note that for small τ_k (e.g., $\tau_k < 0.15$), $F_k \approx \tau_k$.

Nevertheless, a realistic number of 25,000 SNPs (considering currently available data sets in both model and nonmodel species) was sufficient to obtain very satisfactory results on more complex tree topologies, as illustrated in [supplementary figure S2, Supplementary Material](#) online, for six-population trees.

As shown in [figure 4B](#), and in agreement with the above results ([fig. 3B](#)), the different branch lengths were correctly estimated when the analyses were performed conditionally on the correct population tree T1. However, when the analyses were performed conditionally on incorrect tree

topologies (T2 and T3), and although the length of the branch leading to population P3 was correctly estimated, the lengths of the branches leading to P1 and P2 were upwardly biased, and the length of the internal branch (leading to P4) tended toward zero. Therefore, although the method provided correct estimates of the divergence of P3 (the most diverged population in the simulations), all other branch lengths in the population tree were poorly estimated. Interestingly, all else being equal, the internal branch leading to P4 tended to be shrunk, and therefore the lengths of the branches leading to P1, P2, and P3 were close to the values

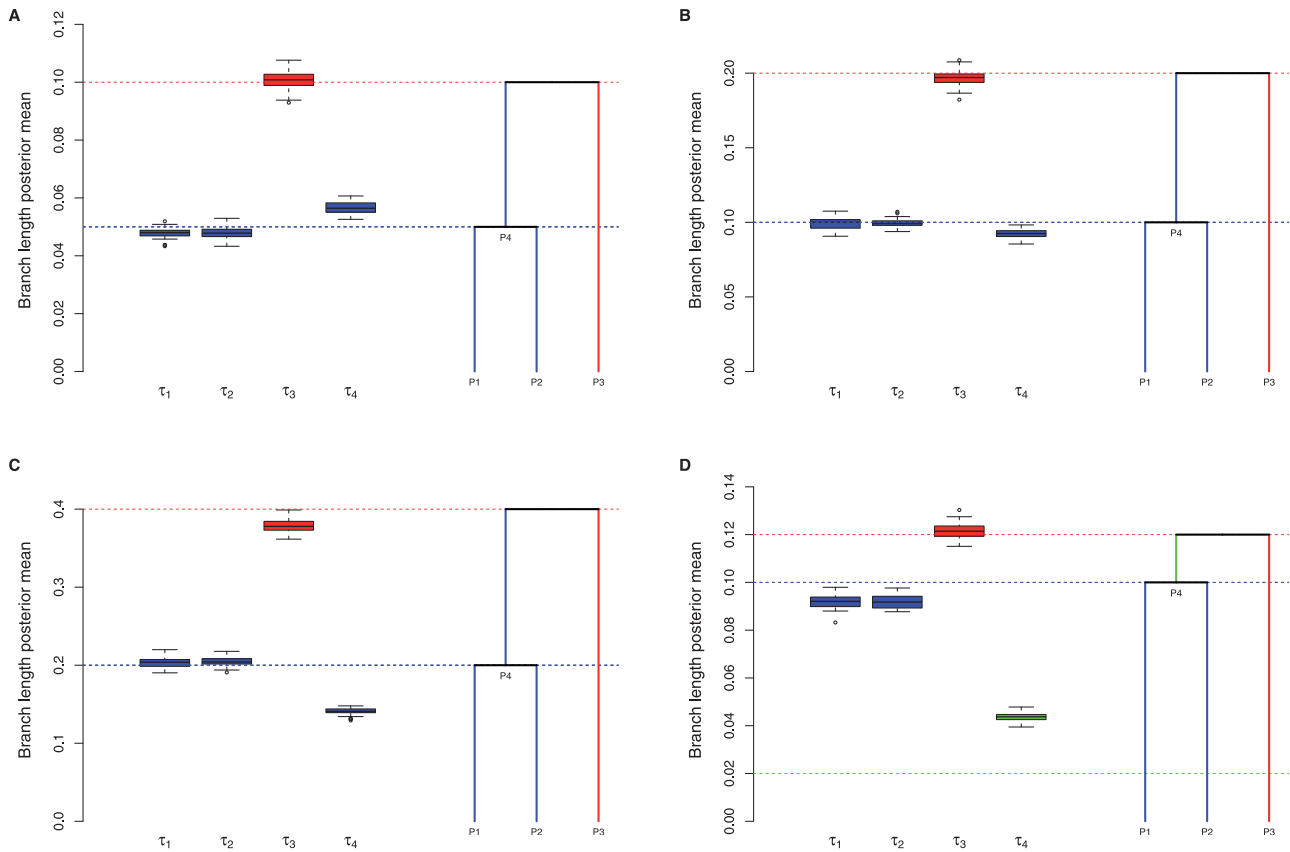


Fig. 3. Performance of the Kimura model for estimating branch lengths in population trees. All histories represented from A to D share the same topology ((P1,P2),P3) but differ in divergence times. For each history, 50 data sets made of 5,000 SNPs were simulated. The boxplots summarize the distributions of the 50 posterior means of τ_k for each of the four branches. The branches are identified by the index of their terminal population, and the horizontal dashed lines indicate the (true) simulated values.

obtained in the analyses run conditionally on a star-shaped population history (S).

Robustness to Model Misspecification

Inference of Branch Lengths in the Presence of Gene Flow

Overall, we found that the DIC always provided a clear support for the correct population tree, across replicated simulated data sets, for low-to-moderate levels of migration ($M = 0.1$ and $M = 1$, table 1) and in most instances (>90%) for a high level of migration ($M = 10$). As for the estimation of branch lengths, we obtained similar results as above when analyzing data sets simulated with a low amount of gene flow between populations ($M = 0.1$, fig. 4C). However, and as expected, increasing the level of migration from moderate ($M = 1$, fig. 4D) to high levels ($M = 10$, fig. 4E) tended to bias downward the branch length estimates. The magnitude of the bias increased with M and was more pronounced for the internal branches. In the most extreme case ($M = 10$, fig. 4E) values, the results obtained conditionally on the correct tree topology (T1) were similar to those obtained conditionally on the incorrect topologies T2, T3, and S.

Inference of Branch Lengths with Ascertained SNPs

To investigate the sensitivity of the Kimura model to ascertainment bias, we simulated data sets based on the three-population history T1 considered earlier. To mimic

ascertainment bias, we defined “ghost” individuals within each of the three sampled populations that were used exclusively for discovery and then discarded from further analyses. We considered three different ascertainment schemes, which differed by the origins of the discovery panels used to ascertain SNPs (see the Material and Methods section). As shown in figure 5A, when the three populations contributed evenly to the SNP discovery panel (ascertainment scheme AS1), we obtained similar results as in the absence of ascertainment bias (compare figs. 4B and 5B). However, we observed a moderate upward bias in the estimate of the branch leading to P3 and a downward bias for the internal branch length estimate (leading to P4), which was larger for analyses performed conditionally on incorrect population histories. When only populations P1 and P3 contributed to the SNP discovery panel (ascertainment scheme AS2), and although the correct population tree was still recognized based on the DIC criterion (table 1), more substantial downward (respectively upward) biases were observed for estimates of the branch lengths leading to P1 and P3 (respectively P2 and P4) (fig. 5C). Finally, when only populations P1 and P2 contributed to the SNP discovery panel (ascertainment scheme AS3), severe biases were observed for estimates of the branch lengths for populations P3 and P4 (fig. 5D). In this latter ascertainment scheme, all else being equal, the branch length estimates were very similar across analyses run with

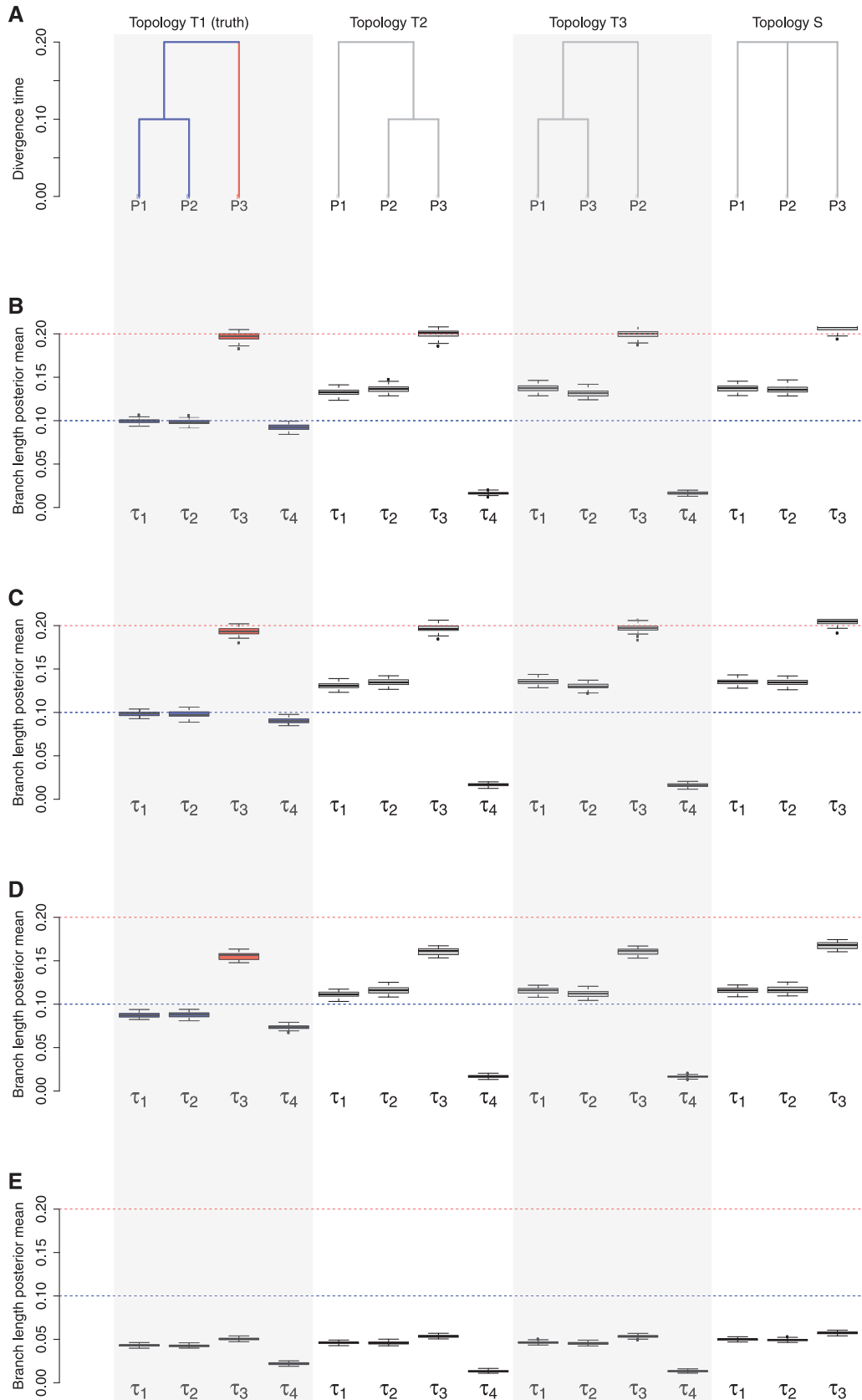


FIG. 4. Performance of the Kimura model for different levels of gene flow and for different underlying topologies. In all cases, data were simulated according to the T1 history, represented at the left-hand side of the upper panel (A). The analyses were then performed conditionally on each of the four possible histories (T1, T2, T3, and S) represented in (A). Four levels of gene flow were considered: $M = 0$ (B), $M = 0.1$ (C), $M = 1$ (D), and $M = 10$ (E). In each case, 50 data sets made of 5,000 SNPs were simulated. The boxplots summarize the distributions of the 50 posterior means of τ_k for each branch. The branches are identified by the index of their terminal population, and the horizontal dashed lines indicate the (true) simulated values.

Table 1. Strength of Evidence for the Different Topologies Considered in Figures 4 and 5, Based on the DIC.

Topology	DIC _{T₂} –DIC _{T₁}		DIC _{T₃} –DIC _{T₁}		DIC _S –DIC _{T₁}	
	Median (Min.; Max.)	<i>n</i> ₁₀	Median (Min.; Max.)	<i>n</i> ₁₀	Median (Min.; Max.)	<i>n</i> ₁₀
Figure 4B (<i>M</i> = 0)	72.0 (45.9; 94.7)	50	68.2 (47.3; 100.6)	50	69.8 (35.9; 94.2)	50
Figure 4C (<i>M</i> = 0.1)	72.7 (44.3; 103.2)	50	73.5 (44.6; 106.1)	50	65.9 (38.5; 107.8)	50
Figure 4D (<i>M</i> = 1)	61.0 (30.7; 87.0)	50	61.5 (33.2; 94.5)	50	57.1 (26.8; 87.0)	50
Figure 4E (<i>M</i> = 10)	26.5 (–13.2; 58.8)	40	27.6 (–5.2; 56.5)	43	30.6 (–0.7; 63.2)	44
Figure 5B (AS1)	65.8 (36.9; 88.5)	50	68.7 (31.4; 97.1)	50	69.7 (36.9; 99.5)	50
Figure 5C (AS2)	81.3 (44.0; 106.6)	50	98.8 (66.4; 126.5)	50	101 (65.5; 135)	50
Figure 5D (AS3)	10.6 (–22.2; 41.8)	25	8.80 (–26.3; 38.2)	22	10.3 (–17.6; 44)	25

NOTE.—The median (minimum; maximum) of the distribution of the difference between the DIC (Δ_{DIC}) of a wrong topology (T2, T3, or S) and the correct one (T1), over 50 replicated simulations, is listed. *n*₁₀ gives the number of simulations (out of 50) where $\Delta_{DIC} > 10$.

Table 2. Effect of the Number of SNPs on the DIC.

Number of SNPs	DIC _{T₂} –DIC _{T₁}		DIC _{T₃} –DIC _{T₁}		DIC _S –DIC _{T₁}	
	Median (Min.; Max.)	<i>n</i> ₁₀	Median (Min.; Max.)	<i>n</i> ₁₀	Median (Min.; Max.)	<i>n</i> ₁₀
1,000	13.6 (0.2; 27)	38	14.3 (2.6; 26.2)	40	14.4 (–7.1; 28.6)	38
5,000	72.0 (45.9; 94.7)	50	68.2 (47.3; 100.6)	50	69.8 (35.9; 94.2)	50
25,000	364.1 (286.8; 451.5)	50	357.3 (306.2; 425.7)	50	338.4 (276.7; 408.9)	50

NOTE.—Data were simulated according to the same history as in figure 3A, with 1,000, 5,000, and 25,000 SNPs. Each column reports the median (minimum; maximum) of the distribution of the difference (Δ_{DIC}) between the DIC of a wrong tree (T2, T3, or S) and the correct one (T1), over 50 replicated simulations. *n*₁₀ gives the number of simulations (out of 50) where $\Delta_{DIC} > 10$.

different prior tree topologies. In particular, the analyses run conditionally on incorrect topologies T2 and T3 provided similar branch length estimates as in the analyses run conditionally on a star-shaped population history (S), with a shrunk internal branch leading to P4. It was only for this ascertainment scheme (AS3) that the DIC failed to support the correct population tree (table 1).

Inference of Branch Lengths in the Presence of Recent Mutations

In SNP genotyping assays, the SNP ascertainment schemes similar to the AS1 and the AS2 schemes ensure that “ancestral” SNPs (i.e., SNPs that predate the divergence of the populations under study) are largely over-represented. An over-representation of ancestral SNPs may also occur if the common ancestral population has undergone a strong bottleneck, as for instance in humans or in most domesticated species. However, overlooking “derived” SNPs (i.e., SNPs that arose after the divergence of the populations under study from the root population) is expected to affect the robustness of our model, if new mutations occur after the split of the most ancestral population.

Removing the bottleneck (i.e., the *-en* option in the *ms* command) in our simulations resulted indeed in higher downward biases for the estimation of branch lengths (supplementary fig. S3, Supplementary Material online) and poorer identification of the correct underlying tree (supplementary table S2, Supplementary Material online) as divergence times increased. However, some ascertainment schemes (particularly AS1) may improve performance probably if they result in an enrichment of the data sets in ancestral SNPs (supplementary fig. S4, Supplementary Material online).

Example Application on a Large Human Data Set

As an illustration example, we ran our model based on Kimura’s diffusion approximation on a large human data set. The data consisted in allele counts at 452,198 autosomal SNPs from four human populations of African (the Yorubas from Nigeria or YRI and the Biaka Pygmies from Congo or BIA), European (the US European American from Utah or CEU), and East Asian (the Japanese or JPT) ancestry (Jakobsson et al. 2008). To evaluate the extent to which summarizing the history of these four populations by a bifurcating tree is not overly simplistic, we first performed four-population tests for treeness (also referred to as quartet tests for migration) on the three possible (labeled) unrooted tree topologies (see Keinan et al. 2007; Reich et al. 2009). As detailed in supplementary table S1, Supplementary Material online, the four-population tests for treeness supported the ((YRI,BIA),(CEU,JPT)) unrooted tree topology ($P < 0.15$) and rejected the two alternative ones ($P < 10^{-20}$). This result is in agreement with Keinan et al. (2007), who considered individuals from the same populations (YRI and CEU) and closely related ones (Mbuti Pygmy and Chinese from Beijing) but a different set of SNPs. This result further suggests that migration between YRI or BIA on the one hand and CEU or JPT on the other hand has been maintained at a low level since the population split and has not seriously distorted the joint allele frequency spectrum.

To infer more precisely the relations between the four worldwide populations YRI, BIA, CEU, and JPT, we then ran our analyses conditionally on six alternative rooted population trees. As represented in figure 6, these trees corresponded to the five possible rooted topologies derived from the ((YRI,BIA),(CEU,JPT)) unrooted topology plus a

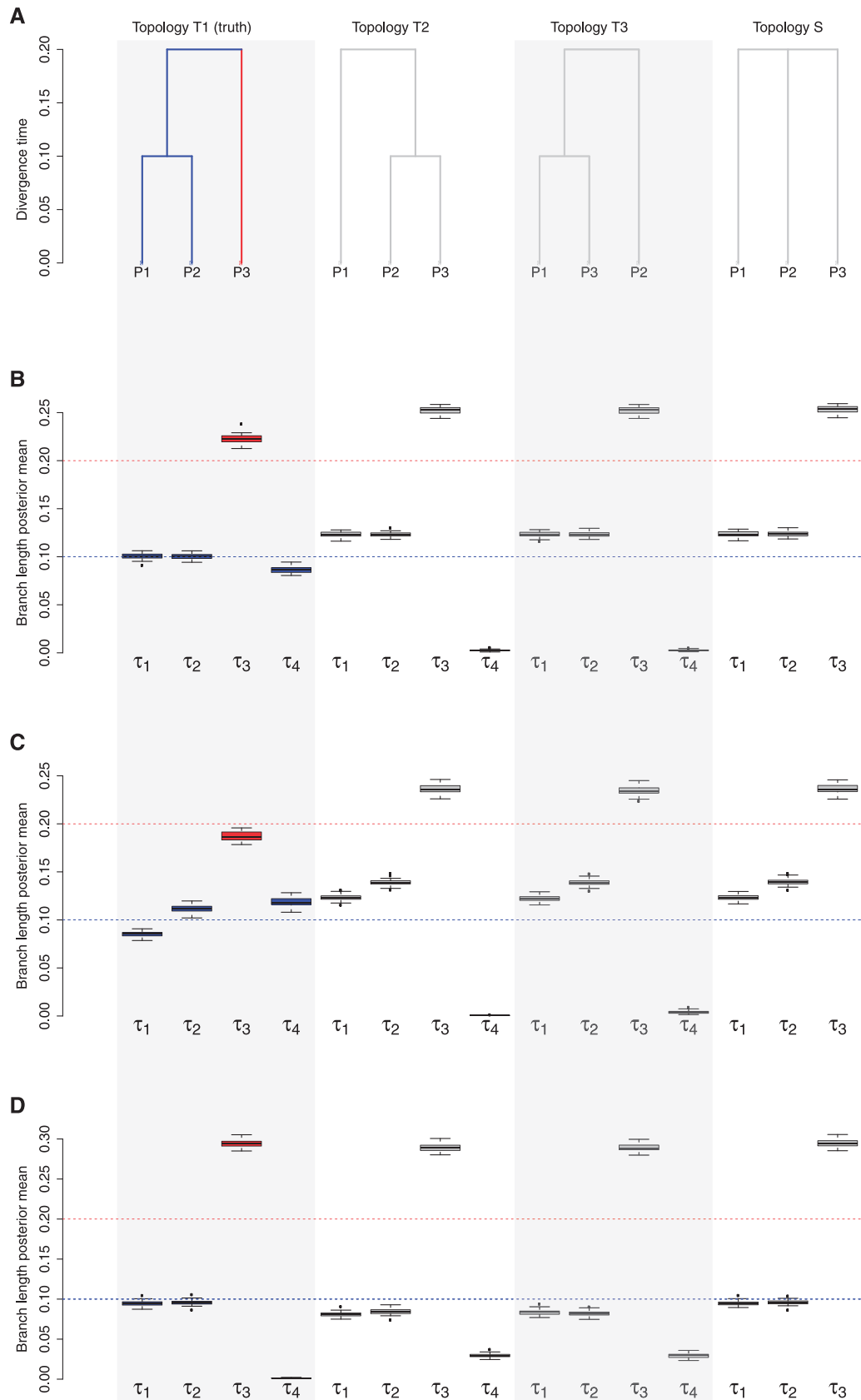


FIG. 5. Performance of the Kimura model for different SNP ascertainment schemes and for different underlying topologies. In all cases, data were simulated according to the T1 history, represented at the left-hand side of the upper panel (A). The analyses were then performed conditionally on each of the four possible histories (T1, T2, T3, and S) represented in (A). Three different SNP ascertainment schemes were considered: AS1 (B), AS2 (C), and AS3 (D) (see the main text for further details on the ascertainment schemes). In each case, 50 data sets made of 5,000 SNPs were simulated. The boxplots summarize the distributions of the 50 posterior means of τ_k for each branch. The branches are identified by the index of their terminal population, and the horizontal dashed lines indicate the (true) simulated values.

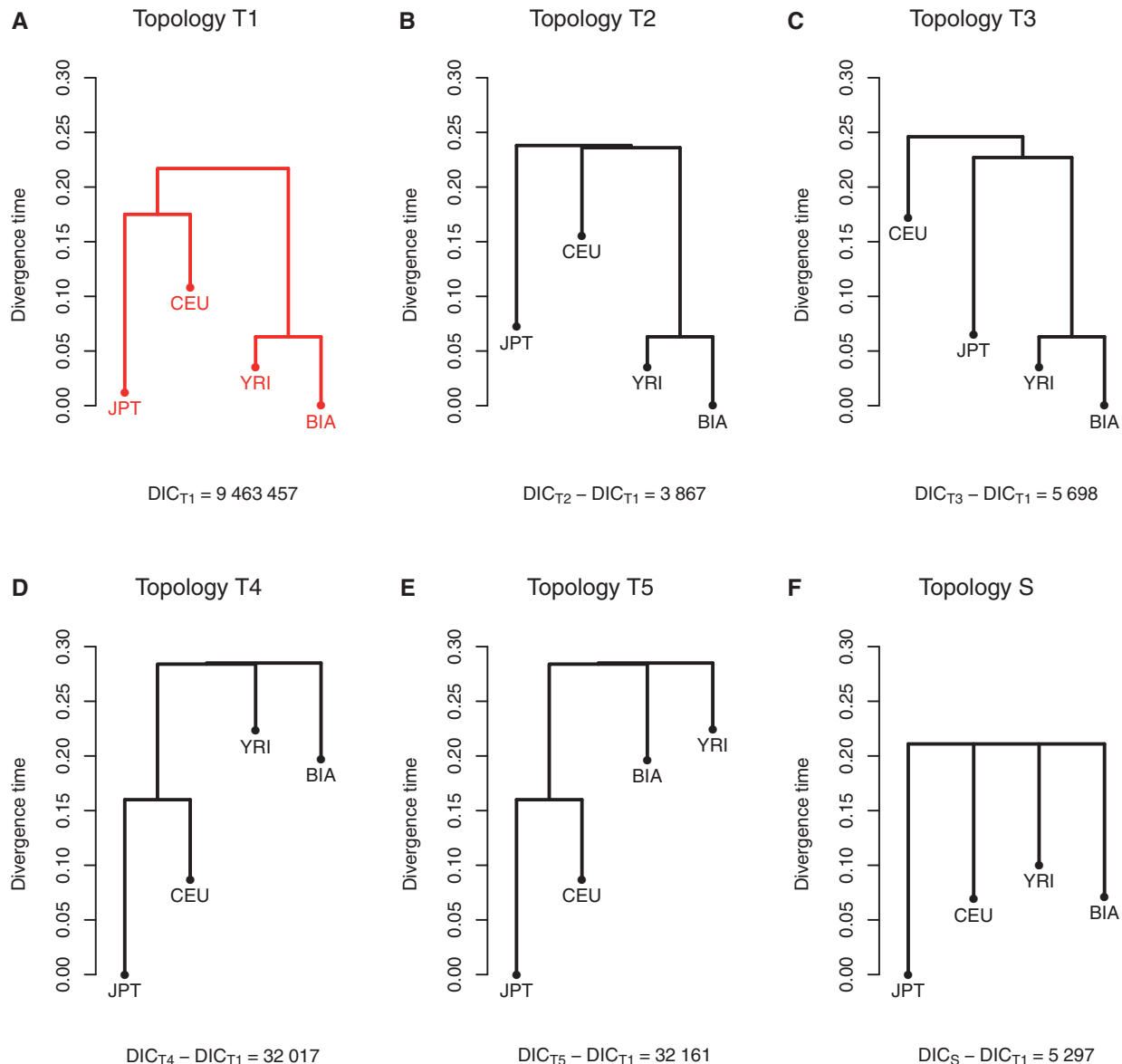


Fig. 6. Estimation of divergence times conditionally on different histories relating four human populations: the Yorubas from Nigeria (YRI), the Biaka Pygmies from Congo (BIA), the US European Americans from Utah with Northern and Western European ancestry (CEU), and the Japanese (JPT). The data set from Jakobsson et al. (2008) consisted in allele counts at 452,198 autosomal SNPs. We analyzed the data using the Kimura model conditionally on five rooted bifurcating topologies (each of which represented from A to E was derived by placing the root on one of the five branches of the most likely unrooted tree, following the four-population test for treeness) and a star phylogeny (F). The estimated posterior means of the divergence time (on a diffusion time scale) are provided for each branch. The topology (A) that received the strongest support based on the DIC is highlighted in red.

star-shaped phylogeny. Based on the DIC criterion, the tree T1 unambiguously received the strongest support, in agreement with the widely accepted Out-Of-Africa model of human evolution.

Discussion

An Efficient Model to Estimate Divergence Times

In this study, we developed a new hierarchical Bayesian model to estimate divergence times (on a diffusion time scale) conditionally on a population tree, using genome-wide allele frequency data. Because genetic drift occurs independently in each branch of the tree in the absence of gene flow, the allele frequency at one particular locus can be modeled

hierarchically along the tree from the most ancestral population toward the leaves. Our model is based on Kimura's diffusion approximation (Kimura 1964), which arises as an explicit solution of the time-dependent Wright-Fisher model. The parameters of interest in this model are the branch lengths, measured as $\tau_k \equiv t/(2N_k)$. This definition calls for two remarks. First, it is evident from Kimura's diffusion approximation that disentangling divergence time t from effective population size N_k is not possible, because of the nonidentifiability of these two parameters. Estimating t , which is generally the parameter of biological interest, would therefore require informative priors on N_k , which in practice can be derived from other analyses (see, e.g., Gautier et al. 2007).

Second, the population size N_k need not be a constant. Indeed, we expect Kimura's diffusion approximation to be robust to the (unknown) demography of the population (see, e.g., Ewens 2004, chapter 5). For instance, with demographic fluctuations, and if we assume that population k has size $N_{k,i}$ in each generation i , then $\tau_k = N_{k,0}^{-1} + \sigma^2 \sum_{i=1}^t N_{k,i}^{-1}$ (see Nicholson et al. 2002), where σ^2 represents the variance in the number of descendant across generations (e.g., $\sigma^2 = 1$ in the Wright–Fisher model).

Not surprisingly, Kimura's diffusion approximation outperforms the two alternative models that have been proposed so far for estimating divergence in star-shaped population histories (Nicholson et al. 2002; Falush et al. 2003; Gautier, Hocking, et al. 2010). One of these alternative models assumed that the allele frequency distribution in each population might be well approximated by a truncated Gaussian distribution (Nicholson et al. 2002), whereas the second model relied on a beta distribution for allele frequencies (Balding and Nichols 1995; Balding 2003). However, neither the truncated Gaussian nor the beta models are based on the analysis of the Wright–Fisher model of genetic drift. Both models are indeed only aimed at modeling the first two moments of the expected distribution of allele frequency, conditionally on the frequency in the ancestral population and the amount of divergence. Note, however, that the beta model (which has been referred to as the F -model by Falush et al. [2003]) arises as the diffusion approximation of genetic drift in the migration-drift equilibrium island model (Balding and Nichols 1995; Balding 2003).

An important difference between the truncated Gaussian and the beta models stems from the fact that only the former allows for variation to be lost in some populations: although the support of the truncated Gaussian is by construction on the $[0, 1]$ real line, the beta model does not include probability masses in 0 and 1 and therefore ignores the possibility of allele loss or fixation. Furthermore, the truncation made on the Gaussian distribution by Nicholson et al. (2002) to account for the masses in 0 and 1 reduces the variance of the distribution of allele frequencies, which becomes rapidly smaller than that expected under pure-drift divergence, as divergence increases and the ancestral allele frequency departs from 0.5 (supplementary fig. S5, Supplementary Material online). Indeed, although the expected variance in the Wright–Fisher model equals $\text{Var}_{\text{WF}} = F\pi(1 - \pi)$, the variance of the truncated Gaussian distribution considered by Nicholson et al. (2002) equals

$$\text{Var} = \left[1 + \frac{a\phi(a) - b\phi(b)}{\Phi(b) - \Phi(a)} - \left(\frac{\phi(a) - \phi(b)}{\Phi(b) - \Phi(a)} \right)^2 \right] \text{Var}_{\text{WF}}, \quad (6)$$

where $a = -\pi/\sqrt{c\pi(1 - \pi)}$ and $b = (1 - \pi)/\sqrt{c\pi(1 - \pi)}$. In equation (6), $\phi(x)$ and $\Phi(x)$ represent, respectively, the probability density function and the cumulative distribution function of the standard normal distribution. The mismatch between the variance of the allele

frequency distribution in the truncated Gaussian model and that expected in the Wright–Fisher model may very well explain the observed upward bias in estimates of divergence with the truncated Gaussian model as divergence time increases (fig. 2).

For all the reasons cited earlier, the Kimura model clearly outperforms the truncated Gaussian and the beta models for the estimation of divergence time under pure-drift scenarios (fig. 2), even for small effective population sizes, over the whole parameter space (supplementary fig. S6, Supplementary Material online). This improved accuracy comes at the expense of computational burden, though, even if the use of a recursive algorithm to estimate the density function was proven to be efficient. For instance, a typical analysis of one of the data sets from figures 3 and 4 (i.e., with 5,000 SNPs and 3 sampled populations, conditionally on a bifurcating tree) took approximately 39 min on a desktop computer equipped with a 3.4 GHz processor. Because computation times are approximately proportional to the product of the number of SNPs and the total number of populations in a given scenario (including internal nodes), analyzing large data sets of several tens to hundreds of thousands SNPs therefore remains tractable even with standard computers.

Providing a prior knowledge on plausible alternative trees (and thus population histories) is available, the DIC model comparison criterion (Spiegelhalter et al. 2002) was proven to be efficient. The DIC had a better behavior than the pseudo Bayes Factor (Gelfand and Dey 1994), another commonly used measure to assess model fit (see supplementary materials, Supplementary Material online, and compare supplementary table S3, Supplementary Material online, and table 2). However, the identification of the correct underlying topology requires, of course, that the correct tree lies among the set of tested trees. As a consequence, our approach might only be viewed as complementary to tree inference methods, to which the two aforementioned approaches proposed by Siren et al. (2011) and Pickrell and Pritchard (2012) belong. Siren's (2011) approach may indeed be used to characterize the posterior optimal tree topology but remains in practice limited to the analysis of a few hundred SNPs due to the computational burden. Similarly, Pickrell and Pritchard's (2012) approach provides a graph representation of the relationships between populations, but because it relies on some extensions of the truncated Gaussian model, it may therefore provide accurate branch length estimates for recent divergences only. In any case, we recommend running three- or four-population tests for treeness (Keinan et al. 2007; Reich et al. 2009), to evaluate the extent to which summarizing a population history by a bifurcating tree is a reasonable assumption (see the example application on a large human data set, earlier).

Influence of Data Set Properties on the Method Performance

Increasing the number of SNPs had generally no effect on the accuracy of branch length estimates. However, based on the

DIC criterion, increasing the number of markers improved substantially the choice of the correct population tree topology. Typically, approximately 5,000 SNPs seemed sufficient to resolve three-population trees in most instances. The number of SNPs required to resolve alternative tree topologies increased with tree complexity, that is, with increasing numbers of sampled populations.

With the recent development of high-throughput genotyping technologies, typical data sets may involve hundreds of thousands of SNPs. In this context, the implicit assumption of conditional independence of markers, which is made in our and others model, and amounts to assume the exchangeability of markers, might be violated. First, the residual linkage disequilibrium (LD) within the genome creates local dependency among neighboring SNPs. The expected squared correlation coefficient r^2 between two SNPs (Hill and Robertson 1968) is well approximated by $E(r^2) \approx 1/\rho$ for large values of the population recombination rate $\rho \equiv 4Nr$, where r represents the frequency of crossing over events per generation (Ohta and Kimura 1969; Sved 1971; McVean 2007). Hence, the extent of pairwise LD declines rapidly toward negligible values as the genetic distance increases, which typically reduces the data to several tens of thousands of “effective” SNPs, as confirmed by empirical studies (see, e.g., Duggal et al. 2008). Although the correlation structure among SNP allele frequencies is not explicitly accounted for in the models, we expect LD to have a limited effect on divergence time estimates in population trees. Nevertheless, LD-based pruning techniques (Purcell et al. 2007), which aim at generating subsets of SNP data in approximate linkage equilibrium, might represent a valuable approach to overcome these difficulties.

Second, the SNP exchangeability assumption also implicitly requires that SNPs are not located within genomic regions targeted by selection. However, the model is expected to remain robust to such departure from neutrality, provided that only a small fraction of SNPs are indeed affected by selective effects (see, e.g., Gautier, Hocking, et al. 2010). Conversely, evaluating the local adjustment of the model at each locus (e.g., using posterior predictive checking) may provide a means to identify outlier SNPs, while simultaneously taking into account the demographic history of the sampled populations (see, e.g., Gautier, Hocking, et al. 2010).

Third, SNP exchangeability requires the absence of ascertainment bias. This assumption is valid for SNP genotyping data sets obtained by means of next-generation sequencing technologies (Baird et al. 2008) but not for SNP genotyping assays, which remain common in most model species. Extending the model to distinguish demographic from ascertainment processes is theoretically possible (Guillot and Foll 2009), although it might lead to additional computational burden in practice. However, our simulation evaluation showed that the Kimura model was robust to ascertainment bias, if the discovery panel was made of individuals sampled from all the populations, or from the most distant populations. This suggests that the discovery panel needs to contain at least some information about the history of the sampled populations as a whole. Both the AS1 and the AS2 ascertainment schemes considered in this study are representative of

the procedures used in humans, which generally rely on the sequencing of a small subset of individuals from very diverse origins. Conversely, when the discovery panel is only made of individuals from the most recently diverged populations (ascertainment scheme AS3), there is virtually no information for the branches issued from the most ancestral population. More generally, our results suggest that demographic inference should be interpreted with caution, and we recommend accounting for SNP ascertainment bias if the analyzed populations are only barely related to the discovery panel. The resulting bias may mainly be related to the over-representation of derived SNPs (i.e., SNPs that did not exist in the most ancestral population) and is therefore expected to be more pronounced if the populations represented in the discovery panel have rapidly expanded since divergence (supplementary fig. S3, Supplementary Material online).

Overlooking derived SNPs is expected to affect the robustness of any inference method based on models that neglect recent mutations (Nicholson et al. 2002; Coop et al. 2010; Gautier, Hocking, et al. 2010; Siren et al. 2011), although this limitation is generally not explicitly stated. New mutations may occur after the split of the most ancestral population, for example, if population sizes are large or if divergence is ancient. Accordingly, the models of population divergence that neglect recent mutations should be used with caution on data sets enriched with derived SNPs.

Finally, we investigated the robustness of our model to departure from pure-drift divergence, by analyzing data sets with simulated with low-to-high levels of gene flow. Interestingly, the correct population tree was generally well supported, even for moderate levels of divergence. Of course, branch lengths were generally biased downward, and the bias increased as the migration rate increased. Alternatively, because of the flexibility of Bayesian hierarchical modeling, it should be straightforward to account (and to test) for admixture in the model by modifying the priors on the ancestral allele frequencies for the presumably admixed populations.

Material and Methods

Parameter Estimation

Our aim is to estimate divergence times (on a diffusion time scale) from genome-wide allele frequency data, conditionally on a population tree from the hierarchical Bayesian model described earlier. To that end, the full posterior distribution of the parameters is estimated by means of a Metropolis–Hastings within Gibbs MCMC algorithm. In this algorithm, each parameter of interest is updated iteratively. The starting values of the chains are taken as standard moment-based estimates of the parameter of interest. At each iteration t of the algorithm, the $I \times J$ parameters α_{ik} (for $k \leq J$), the $I \times (r - J)$ parameters α_{ik} (for $J < k < r$), the I parameters α_{ir} and the $(r - 1)$ parameters τ_k are successively updated in that order, following the steps briefly described in the supplementary materials, Supplementary Material online.

In practice, to deal with probability masses in $\alpha_{ik} = 0$ and $\alpha_{ik} = 1$, we introduced a latent (continuous) variable β_{ik} with support $[-1, 2]$, so that $\alpha_{ik} = \min(1, \max(0, \beta_{ik}))$. The model was then redefined using β_{ik} with probability density function $\pi(\beta_{ik} | \alpha_{ia(k)}, \tau_k)$:

$$\begin{cases} \pi(\beta_{ik} | \alpha_{ia(k)}, \tau_k) = P(\alpha_{ik} = 0 | \alpha_{ia(k)}, \tau_k) & \text{if } -1 \leq \beta_{ik} \leq 0 \text{ and } \alpha_{ia(k)} \in (0, 1) \\ \pi(\beta_{ik} | \alpha_{ia(k)}, \tau_k) = \pi(\alpha_{ik} | \alpha_{ia(k)}, \tau_k) & \text{if } 0 < \beta_{ik} < 1 \text{ and } \alpha_{ia(k)} \in (0, 1) \\ \pi(\beta_{ik} | \alpha_{ia(k)}, \tau_k) = P(\alpha_{ik} = 1 | \alpha_{ia(k)}, \tau_k) & \text{if } 1 \leq \beta_{ik} \leq 2 \text{ and } \alpha_{ia(k)} \in (0, 1) \\ \pi(\beta_{ik} | \alpha_{ia(k)} = 0, \tau_k) = 1 & \text{if } \beta_{ik} \leq 0 \\ \pi(\beta_{ik} | \alpha_{ia(k)} = 0, \tau_k) = 0 & \text{if } \beta_{ik} > 0 \\ \pi(\beta_{ik} | \alpha_{ia(k)} = 1, \tau_k) = 1 & \text{if } \beta_{ik} \geq 1 \\ \pi(\beta_{ik} | \alpha_{ia(k)} = 1, \tau_k) = 0 & \text{if } \beta_{ik} < 1. \end{cases} \quad (7)$$

The proposal distributions for the Metropolis–Hastings updates of the parameters β_{ij} and τ_j are provided in the [supplementary materials, Supplementary Material](#) online. To achieve good convergence of the MCMC, these proposal distributions were adjusted during pilot runs (typically, 25 runs of 1,000 steps were run for each Markov chain). After each pilot run, the proposals were adjusted to increase or decrease the acceptance rate, to obtain acceptance rates lying between 0.2 and 0.4 (Gilks et al. 1996). Then, each MCMC was run for 25,000 iterations after a 5,000 iterations burn-in period. Samples were taken from the chain every 25 iterations (thinning) to reduce autocorrelations. A Fortran executable implementing the MCMC algorithm is available for download at http://mbb.univ-montp2.fr/MBB/uploads/kim_tree.tar.gz (last accessed December 3, 2012).

Model Assessment

Because the tree topology is usually unknown, we were interested in characterizing, for a given data set, the strength of evidence for alternative tree topologies. To do so, we used the DIC, which is a standard criterion for model selection among a finite set of models (Spiegelhalter et al. 2002). It relies on a measure of deviance defined as $D = -2\log(\pi(\mathbf{y} | \theta)) + 2\log(\pi(\mathbf{y}))$, where $\log(\pi(\mathbf{y} | \theta))$ represents the log likelihood of the data \mathbf{y} under the model specified by the parameters θ , and $\pi(\mathbf{y})$ is some fully specified standardizing term, which is function of the data alone. The DIC is then defined as $\text{DIC} = \bar{D} + p_D = 2\bar{D} - D(\bar{\theta})$, where \bar{D} is the posterior mean deviance, which can be interpreted as a Bayesian measure of fit. The effective dimension of the hierarchical model p_D is such that $p_D = \bar{D} - D(\bar{\theta})$, where $D(\bar{\theta})$ is the Bayesian deviance evaluated at the posterior mean of the parameters θ . A DIC difference larger than 10 units between any two models is generally regarded as strong evidence (in term of predictive ability) in favor of the model with the smallest DIC. Here, the data \mathbf{y} correspond to the allele counts $\{x_{ij}\}$, and the parameters θ correspond to the subset of parameters in the hierarchical models, upon which the data immediately depend, that is, the α_{ij} s with $1 \leq j \leq J$. Because the latter parameters are not straightforward to

integrate out (see earlier and [supplementary materials, Supplementary Material](#) online), the DIC was simply computed as:

$$\begin{aligned} \text{DIC} = & \frac{2}{T} \sum_{t=1}^T \sum_{i=1}^I \sum_{j=1}^J \log \left[\binom{n_{ij}}{x_{ij}} \alpha_{ij}(t)^{x_{ij}} (1 - \alpha_{ij}(t))^{n_{ij} - x_{ij}} \right] \\ & - \sum_{i=1}^I \sum_{j=1}^J \log \left[\binom{n_{ij}}{x_{ij}} \bar{\alpha}_{ij}^{x_{ij}} (1 - \bar{\alpha}_{ij})^{n_{ij} - x_{ij}} \right]. \end{aligned} \quad (8)$$

In equation (8), $\alpha_{ij}(t)$ is the t th sampled value of the parameter α_{ij} along the MCMC, out of a total of T value, and $\bar{\alpha}_{ij} = \frac{1}{T} \sum_{t=1}^T \alpha_{ij}(t)$ is the posterior mean of α_{ij} .

Simulated Data Sets

To analyze the precision of our model for estimating the level of differentiation over generations, relatively to the beta (Balding and Nichols 1995) and the truncated Gaussian (Nicholson et al. 2002) models, we used a Wright–Fisher forward-in-time simulation algorithm consisting in successive binomial sampling over generations, as described in Gautier, Hocking, et al. (2010). In these simulations, we considered four populations diverging simultaneously from a single ancestral population (star-shaped history), each made of 1,000 haploid individuals. We simulated 5,000 SNPs, and the initial reference allele frequencies (in the most ancestral population) were sampled from a uniform distribution: $\mathcal{U}(0.001, 0.999)$. The sample sizes were set to 100 genes per population to allow the accurate estimation of population differentiation parameters in the first generations ($t < 50$). All SNPs were retained in that set of simulations, even if fixed.

To test the performance of our model in more general settings, we performed additional stochastic simulations, independent from the model assumptions. To that end, simulations were carried out using the coalescent algorithm implemented in the *ms* software package (Hudson 2002). We used the `-s` option, which randomly puts a single mutation on the simulated genealogies. Each of these simulated data sets also consisted in 5,000 SNPs, genotyped in 50 diploid individuals (100 genes) per population. As an example, for the tree topology described in [figure 3B](#), which assumes that P1 and P2 derived from population P4 $\tau_1 = \tau_2 = 0.1$ units of time ago (on a diffusion time scale) and that P3 and P4 derived from the most ancestral one $\tau_3 = 0.2$ and $\tau_4 = 0.1$ units of time ago, respectively, we used the following *ms* command line:

```
ms 300 5000 -l 3 100 100 100 0 -ej 0.05 2 1 -ej 0.1 3 1 -en 0.1 1 25 -s 1.
```

Note that we assumed that the most ancestral (root) population went through a bottleneck before splitting into P3 and P4, to limit the occurrence of SNPs that arose after the divergence of the populations under study from the most ancestral (root) population (see earlier), which were referred to as derived SNPs.

We then investigated the sensitivity of our model to mis-specification, in particular in the presence of gene flow, ascertainment bias, and derived SNPs. We tested the effect

of model misspecification both on model choice (when comparing alternative tree topologies) and branch length estimates. We first examined the consequence of gene flow on the inference of population histories. To that end, we introduced a migration parameter $M \equiv 4Nm$ (where m represents the immigration rate in each generation along the simulated tree). Four values were investigated, namely $M = 0$ (corresponding to the simulation model earlier), $M = 0.1$ (slight departure from the pure-drift model), $M = 1$ (moderate departure), and $M = 10$ (strong departure).

The analysis of SNP data is usually complicated by the discovery protocols applied to ascertain SNPs. Typically, SNPs are called from the genetic material of a small sample of individuals, referred to as the discovery panel. Only then are the ascertained SNPs genotyped in the samples of interest. This procedure results in samples that contain less alleles at low frequency than expected in the absence of ascertainment (Nielsen 2000). To analyze the consequences of SNP ascertainment bias on the inference of divergence times, we simulated SNP data sets mimicking different ascertainment schemes. For that purpose, we simulated three-population trees with the *ms* program, introducing diploid “ghost” individuals that were used exclusively for discovery and then discarded from further analyses. Three different ascertainment schemes were considered. In the first (AS1), SNPs were retained if polymorphic in the six ghost individuals (12 genes) originating from P1, P2, and P3. In the second (AS2), SNPs were retained if polymorphic in the four ghost individuals (8 genes) originating from P1 and P3. In the third (AS3), SNPs were retained if polymorphic in the four ghost individuals originating from P1 and P2.

Real Data Set

As an illustrative example, we analyzed a subset of the human data from Jakobsson et al. (2008) consisting in allele counts at 452,198 autosomal SNPs from four human populations: the Yorubas from Nigeria (YRI, $2n = 72$), the Biaka Pygmies from Congo (BIA, $2n = 64$), the US European Americans from Utah with Northern and Western European ancestry (CEU, $2n = 96$), and the Japanese (JPT, $2n = 32$). The 452,198 SNPs that we retained from the total data set fulfilled the following conditions: 1) to pass the quality check performed by Jakobsson et al. (2008), 2) to be polymorphic in the total pooled sample, and 3) to be genotyped in at least 95% of individuals from each population.

Supplementary Material

Supplementary materials, figures S1–S6, and tables S1–S3 are available at *Molecular Biology and Evolution* online (<http://www.mbe.oxfordjournals.org/>).

Acknowledgments

The authors thank Khalid Belkhir and Remy Derna (Institut des Sciences de l'Évolution, Montpellier) for making the program available in the MBB platform (<http://mbb.univ-montp2.fr/MBB/index.php>, last accessed December 3, 2012). They are grateful to three anonymous reviewers for their

helpful suggestions and corrections. This work was supported, in part, by the French Agence Nationale de la Recherche (grant number 09-BLAN-0145-01).

References

- Alexander DH, Novembre J, Lange K. 2009. Fast model-based estimation of ancestry in unrelated individuals. *Genome Res.* 19:1655–1664.
- Baird NA, Etter PD, Atwood TS, Currey MC, Shiver AL, Lewis ZA, Selker EU, Cresko WA, Johnson EA. 2008. Rapid SNP discovery and genetic mapping using sequenced RAD markers. *PLoS One* 3:e3376.
- Balding DJ. 2003. Likelihood-based inference for genetic correlation coefficients. *Theor Popul Biol.* 63:221–30.
- Balding DJ, Nichols RA. 1995. A method for quantifying differentiation between populations at multi-allelic loci and its implications for investigating identity and paternity. *Genetica* 96:3–12.
- Beaumont M. 2008. Joint determination of topology, divergence time, and immigration in population trees. In: Matsumura S, Forster P, Renfrew C, editors. *Simulations, genetics, and human prehistory*. Cambridge (UK): McDonald Institute for Archaeological Research. p. 135–154.
- Cavalli-Sforza LL, Edwards AW. 1967. Phylogenetic analysis. Models and estimation procedures. *Am J Hum Genet.* 19:233–257.
- Coop G, Witonsky D, Rienzo AD, Pritchard JK. 2010. Using environmental correlations to identify loci underlying local adaptation. *Genetics* 185:1411–1423.
- Crow JF, Kimura M. 1971. *An introduction to population genetics theory*. Caldwell (NJ): Blackburn Press.
- Duggal P, Gillanders EM, Holmes TN, Bailey-Wilson JE. 2008. Establishing an adjusted p-value threshold to control the family-wide type 1 error in genome wide association studies. *BMC Genomics* 9:516.
- Ewens WJ. 2004. *Mathematical population genetics*. 2nd ed. New York: Springer.
- Excoffier L. 2007. Analysis of population subdivision, chapter 29. In: Balding DJ, Bishop M, Cannings C, editors. *Handbook of statistical genetics*, 3rd ed. Chichester (UK): Wiley. p. 980–1020.
- Falush D, Stephens M, Pritchard JK. 2003. Inference of population structure using multilocus genotype data: linked loci and correlated allele frequencies. *Genetics* 164:1567–1587.
- Felsenstein J. 2003. *Inferring phylogenies*. 2nd ed. Sunderland (MA): Sinauer Associates.
- Gautier M, Faraut T, Moazami-Goudarzi K, et al. (12 co-authors). 2007. Genetic and haplotypic structure in 14 European and African cattle breeds. *Genetics* 177:1059–1070.
- Gautier M, Hocking TD, Foulley JL. 2010. A Bayesian outlier criterion to detect SNPs under selection in large data sets. *PLoS One* 5:e11913.
- Gautier M, Laloë D, Moazami-Goudarzi K. 2010. Insights into the genetic history of French cattle from dense SNP data on 47 worldwide breeds. *PLoS One* 5:e13038.
- Gelfand AE, Dey DK. 1994. Bayesian model choice: asymptotics and exact calculations. *J Roy Stat Soc B.* 56:501–514.
- Gilks WR, Richardson S, Spiegelhalter DJ. 1996. *Markov Chain Monte Carlo in practice*. London: Chapman Hall.
- Guillot G, Foll M. 2009. Correcting for ascertainment bias in the inference of population structure. *Bioinformatics* 25:552–554.
- Gutenkunst RN, Hernandez RD, Williamson SH, Bustamante CD. 2009. Inferring the joint demographic history of multiple populations from multidimensional SNP frequency data. *PLoS Genet.* 5:e1000695.

- Hein J, Schierup MH, Wiuf C. 2005. Gene genealogies, variation and evolution: a primer in coalescent theory, 1st edn. Oxford University Press.
- Hey J, Nielsen R. 2004. Multilocus methods for estimating population sizes, migration rates and divergence time, with applications to the divergence of *Drosophila pseudoobscura* and *D. persimilis*. *Genetics* 167:747–760.
- Hey J, Nielsen R. 2007. Integration within the Felsenstein equation for improved Markov chain Monte Carlo methods in population genetics. *Proc Natl Acad Sci U S A*. 104:2785–2790.
- Hill WG, Robertson A. 1968. Linkage disequilibrium in finite populations. *Theor Appl Genet*. 38:226–231.
- Hudson RR. 2002. Generating samples under a Wright-Fisher neutral model of genetic variation. *Bioinformatics* 18:337–338.
- Jakobsson M, Scholz SW, Scheet P, et al. (24 co-authors). 2008. Genotype, haplotype and copy-number variation in worldwide human populations. *Nature* 451:998–1003.
- Jombart T, Pontier D, Dufour AB. 2009. Genetic markers in the playground of multivariate analysis. *Heredity* 102:330–341.
- Keinan A, Mullikin JC, Patterson N, Reich D. 2007. Measurement of the human allele frequency spectrum demonstrates greater genetic drift in East Asians than in Europeans. *Nat Genet*. 39:1251–1255.
- Kijas JW, Lenstra JA, Hayes B, et al. (17 co-authors). 2012. Genome-wide analysis of the world's sheep breeds reveals high levels of historic mixture and strong recent selection. *PLoS Biol*. 10:e1001258.
- Kimura M. 1964. Diffusion models in population genetics. *J Appl Probab*. 1:177–232.
- Kingman JFC. 1982. On the genealogy of large populations. *J Appl Probab*. 19:27–43.
- Li JZ, Absher DM, Tang H, et al. (11 co-authors). 2008. Worldwide human relationships inferred from genome-wide patterns of variation. *Science* 319:1100–1104.
- Marjoram P, Tavaré S. 2006. Modern computational approaches for analysing molecular genetic variation data. *Nat Rev Genet*. 7: 759–770.
- McVean G. 2007. Linkage disequilibrium, recombination and selection, chapter 27. In: Balding DJ, Bishop M, Cannings C, editors. *Handbook of statistical genetics*. 3rd ed. Chichester (UK): Wiley. p. 909–944.
- McVean G. 2009. A genealogical interpretation of principal components analysis. *PLoS Genet*. 5:e1000686.
- Nicholson G, Smith AV, Jonsson F, Gustafsson O, Stefansson K, Donnelly P. 2002. Assessing population differentiation and isolation from single-nucleotide polymorphism data. *J Roy Stat Soc B*. 64: 695–715.
- Nielsen R. 2000. Estimation of population parameters and recombination rates from single nucleotide polymorphisms. *Genetics* 154: 931–942.
- Novembre J, Johnson T, Bryc K, et al. (12 co-authors). 2008. Genes mirror geography within Europe. *Nature* 456:98–101.
- Ohta T, Kimura M. 1969. Linkage disequilibrium at steady state determined by random genetic drift and recurrent mutation. *Genetics* 63: 229–238.
- Patterson N, Price AL, Reich D. 2006. Population structure and eigenanalysis. *PLoS Genet*. 2:e190.
- Pickrell J, Pritchard JK. 2012. Inference of population splits and mixtures from genome-wide allele frequency data. *PLoS Genet*. 8:e1002967.
- Pritchard JK, Stephens M, Donnelly P. 2000. Inference of population structure using multilocus genotype data. *Genetics* 155:945–959.
- Purcell S, Neale B, Todd-Brown K, et al. (11 co-authors). 2007. PLINK: a tool set for whole-genome association and population-based linkage analyses. *Am J Hum Genet*. 81:559–575.
- Reich D, Thangaraj K, Patterson N, Price AL, Singh L. 2009. Reconstructing Indian population history. *Nature* 461:489–494.
- Saitou N, Nei M. 1987. The neighbor-joining method: a new method for reconstructing phylogenetic trees. *Mol Biol Evol*. 4:406–425.
- Siren J, Marttinen P, Corander J. 2011. Reconstructing population histories from single nucleotide polymorphism data. *Mol Biol Evol*. 28: 673–683.
- Spiegelhalter DJ, Best NG, Carlin BP, Linde AVD. 2002. Bayesian measures of model complexity and fit. *J Roy Stat Soc B*. 64:583–639.
- Sved J. 1971. Linkage disequilibrium and homozygosity of chromosome segments in finite populations. *Theor Popul Biol*. 2:125–141.
- Tang H, Peng J, Wang P, Risch NJ. 2005. Estimation of individual admixture: analytical and study design considerations. *Genet Epidemiol*. 28: 289–301.
- Wakeley J. 2008. *Coalescent theory: an introduction*. 1st ed. Greenwood Village (CO): Roberts Company Publishers.
- Wang Y, Nielsen R. 2012. Estimating population divergence time and phylogeny from single-nucleotide polymorphisms data with out-group ascertainment bias. *Mol Ecol*. 21:974–986.
- Wang Y, Rannala B. 2004. A novel solution for the time-dependent probability of gene fixation or loss under natural selection. *Genetics* 168:1081–1084.
- Weir BS, Hill WG. 2002. Estimating F-statistics. *Annu Rev Genet*. 36: 721–750.
- Wright S. 1969. *Evolution and the genetics of populations, volume 2: theory of gene frequencies*. 1st ed. Chicago: University of Chicago Press.